Dynamic Legged Ball Manipulation on Rugged Terrains with Hierarchical Reinforcement Learning

***Abstract*—Advancing the dynamic loco-manipulation capabilities of quadruped robots in complex terrains is crucial for performing diverse tasks. Specifically, dynamic ball manipulation in rugged environments presents two key challenges. The first is coordinating distinct motion modalities to integrate terrain traversal and ball control seamlessly. The second is overcoming sparse rewards in end-to-end reinforcement learning, which impedes efficient policy convergence. To address these challenges, we propose a hierarchical reinforcement learning framework. A high-level policy, informed by proprioceptive data and ball position, adaptively switches between pre-trained low-level skills such as ball dribbling and rough terrain navigation. We further propose Dynamic Skill-Focused Policy Optimization to suppress gradients from inactive skills and enhance critical skill learning. Both simulation and real-world experiments validate that our methods outperform baseline approaches in dynamic ball manipulation across rugged terrains, highlighting its effectiveness in challenging environments.**

***Index Terms*—Reinforcement learning, hierarchical control, loco-manipulation, quadruped robots.**

I. Introduction

WITH rapid advances in robotics and AI, quadruped robots can perform agile movements such as running [1], parkour [2], and football shooting [3], showing great potential in various practical applications. Currently, loco-manipulation—manipulating objects while executing dynamic movements—remains a central challenge [4]. By reusing the legs for manipulation, loco-manipulation enhances the multi-tasking ability of quadruped robots and reduces operational costs. This capability is crucial for tasks such as search-and-rescue, package delivery, and robot soccer competitions. Ball manipulation, as a canonical benchmark for such loco-manipulation tasks, has received extensive research attention in recent years [5], [6].

As a dynamic mobile manipulation task, ball manipulation necessitates a seamless integration of visual perception, dynamic locomotion, and object manipulation. DribbleBot [5] trains in simulation with reinforcement learning (RL) and domain randomization, demonstrating its ability to perform zero-shot transfer to dribble the ball on flat ground. DexDribbler [6] adds a reward term for feedback control and a context-aided estimator to strengthen ball control. However, these works lack the capability to both traverse complex terrains and manipulate dynamic objects on rugged surfaces.

Extending dribbling from flat ground to rugged terrain is not merely a matter of improving robustness; it introduces a fundamental challenge. The task is inherently hybrid, requiring seamless switching between two distinct motion modalities—one centered on terrain traversal that prioritizes the robot's own stability, and the other centered on manipulation that demands precise control of an external object. These modalities impose conflicting requirements on the control policy, making a single end-to-end RL approach difficult to train effectively and prone to impaired convergence. To address the hybrid dynamics and conflicting objectives, we advocate decomposing the problem. We propose a hierarchical reinforcement learning (HRL) framework in which a high-level policy learns to coordinate a set of pre-trained, task-specialized low-level skills (e.g., dribbling and rough-terrain locomotion) to efficiently accomplish dynamic dribbling over complex terrains.

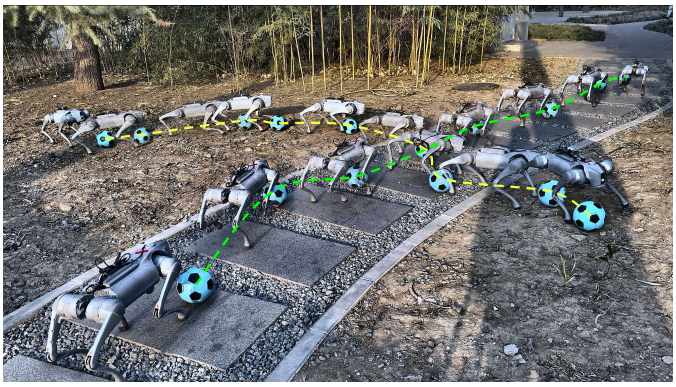

Fig. 1. **Experiments on dynamic ball dribbling over rugged terrains.** The green trajectory traces downhill dribbling over stone slabs and loose gravel; the yellow trajectory shows dribbling across a mixed surface of wet mud, raised curbs, stone slabs, and loose gravel.

This paper aims to design an efficient learning framework for legged ball manipulation on rugged terrains. The main challenge is that ball manipulation and locomotion on rugged terrains are two *distinct motion modalities* that cannot be addressed by the same control strategy [7]. Additionally, end-to-end RL approach [5], [6] struggles to provide useful reward signals for the initial policy on such terrain, thereby inhibiting exploration. To solve these problems, we adopt HRL, integrating policies for both ball dribbling and terrain traversal (Fig. 1). The high-level policy perceives the terrain and ball position in real time, enabling agile switching between low-level dribbling and locomotion skills to maintain ball control. To address learning efficiency and convergence challenges in mixed discrete-continuous action spaces for this task, we propose a dynamic skill-focused loss formulation by suppressing gradients from inactive skills and amplifying critical ones, improving convergence and stability. Furthermore, reward design and curriculum learning are used to improve training, boosting policy convergence and task completion.

The main contributions of our work are as follows:

1) A hierarchical RL framework for agile control over low-level skills to achieve dynamic ball manipulation on rugged terrains.

2) A novel loss formulation, Dynamic Skill-Focused Policy Optimization (DSF-PO), designed for handling the simultaneous discrete and continuous outputs of the high-level policy.
3) Demonstration of ball manipulation on rugged terrains in simulation and successful transfer to a real-world robot.

II. Related Work

A. Locomotion and Manipulation with Quadruped Robots

Recent advances in learning-based methods have enabled quadruped robots to perform increasingly complex locomotion and manipulation tasks [1], [8]–[15]. A dominant paradigm is training controllers in physics simulators, often with large-scale GPU parallelism, and subsequently deploying them in the real world [16]–[20]. For manipulation, learning-based approaches typically generate end-effector trajectories [21], [22] or learn policies directly. Trajectory-following methods, for instance, often use RL-based motion tracking networks to follow Bezier curves generated by a high-level planner [3], [23]–[25]. For more dynamic tasks like in-motion ball dribbling, direct RL optimization with techniques such as domain randomization has been explored [5], [6].

However, these methods have primarily focused on flat-ground scenarios. Robustly integrating dynamic locomotion with precise manipulation to achieve tasks like dribbling on complex, rugged terrains remains a significant challenge. This motivates our approach to develop a unified framework that seamlessly integrates locomotion and dribbling strategies.

B. Hierarchical RL for Robot Control

HRL frameworks, such as the options framework [26] and goal-conditioned hierarchies [27], are a natural paradigm for such complex tasks, offering advantages in exploration and long-horizon credit assignment [28]. In robotics, these frameworks are primarily classified into two categories. The first approach utilizes a task-independent low-level controller, which can be a learning-based trajectory tracker [24], [25], [29], [30] or a model-based generator [31]. This low-level controller is commanded by a task-specific high-level policy that provides either goal positions [32], [33] or trajectory parameters [3], [23]. The second category focuses on integrating multiple specialized skills. For instance, some works incorporate diverse skills using residual modules [34], [35], while others suggest that different skills can specialize in distinct behaviors and be composed, akin to a mixture-of-experts [7].

Inspired by hierarchical control frameworks that leverage both task decomposition and multi-skill integration, we adopt this approach for legged ball dribbling. By leveraging a hierarchical structure, our method ensures flexible skill coordination and enhances adaptability to diverse environments.

III. Methodology

A. Problem Formulation

We model cross-terrain dribbling as a partially observable Markov decision process (POMDP):

$$\mathcal{M} = (\mathcal{S}, \mathcal{A}, \mathcal{O}, \mathcal{T}, \mathcal{R}, \gamma), \quad \mathbf{o}_t = \Phi(\mathbf{s}_t) \in \mathcal{O},\ \mathbf{a}_t \in \mathcal{A}, \quad (1)$$

with state $\mathbf{s}_t = (\mathbf{x}_t^r, \mathbf{x}_t^b, \eta_t) \in \mathcal{S}$, where $\mathbf{x}_t^r$ is the robot state, $\mathbf{x}_t^b = (\mathbf{p}_t^{\text{ball}}, \mathbf{v}_t^{\text{ball}})$ the ball state, and η_t a terrain embedding. Contact modality between robot and ball is distinguished by the impulse indicator

$$i_t \triangleq \mathbf{1}(\|\mathbf{J}_t\| > 0) \in \{0, 1\}, \quad (2)$$

where $\mathbf{J}_t$ denotes the net robot–ball impulse on the ball over $(t-\Delta t/2, t+\Delta t/2)$. This indicator is zero in the case of *non-contact* (nc) and one upon *contact* (c). The transition kernel decomposes by contact modality as

$$\mathcal{T}(\mathbf{s}_{t+1} \mid \mathbf{s}_t, \mathbf{a}_t) = \begin{cases} \mathcal{T}_{\text{nc}}(\mathbf{s}_{t+1} \mid \mathbf{s}_t, \mathbf{a}_t), & i_t = 0, \\ \mathcal{T}_{\text{c}}(\mathbf{s}_{t+1} \mid \mathbf{s}_t, \mathbf{a}_t), & i_t = 1, \end{cases} \quad (3)$$

characterized by the ball-velocity update‘ law:

$$\begin{cases} \mathbf{v}_t^{b,+} = \mathbf{v}_t^{b,-} + \boldsymbol{\varepsilon}_t, & \text{nc } (i_t = 0), \\ \mathbf{v}_t^{b,+} = \mathbf{v}_t^{b,-} + m_b^{-1}\,\mathbf{J}_t, & \text{c } (i_t = 1), \end{cases} \quad (4)$$

where m_b is the ball mass and $v_t^{b,-}, v_t^{b,+}$ are the pre- and post-impact ball velocities. Since $\mathcal{T}_{\text{nc}}$ and $\mathcal{T}_{\text{c}}$ differ in their dynamics, the two modalities are treated as distinct regimes within the formulation while sharing the same observation and action spaces. The objective of policy π is

$$J(\pi) = \mathbb{E}\left[\sum_{t=0}^{\infty} \gamma^t\, \mathcal{R}(\mathbf{s}_t, \mathbf{a}_t)\right]. \quad (5)$$

B. Hierarchical Policy Architecture

To address the hybrid dynamics discussed above, we propose a novel hierarchical framework depicted in Fig. 2. This architecture is composed of two layers: a library of pre-trained low-level skills that execute fundamental behaviors, and a high-level policy that learns to coordinate them.

1) Low-level Skills: The foundation of our framework is a set of four pre-trained, specialized low-level skills that tackle the distinct motion modalities of the task. Specifically, two dribbling skills perform dribbling when the ball is nearby (corresponding to $\mathcal{T}_{\text{c}}$), whereas two locomotion skills handle rapid ball approaching from a distance or traversing rough terrains (corresponding to $\mathcal{T}_{\text{nc}}$). They serve as a modular library of primitive actions for the high-level policy to compose.

- Dribbling Skills (π_1^L, π_2^L): These skills are designed to handle the contact modality. Their objective is to use the robot's front limbs to impart an appropriate impulse to the ball, so that it rolls with a prescribed direction and speed. We train these skills with PPO [36] in Isaac Gym [37] under a flat-terrain setting. The training setup for the dribbling skills adopts similar designs inspired by prior work, with π_1^L following [5] and π_2^L following [6]. Specifically, π_1^L executes a stronger kick, while π_2^L applies a gentler kick and consequently achieves a smaller turning radius.
- Locomotion Skills (π_3^L, π_4^L): These skills address the non-contact modality, aiming to enable the robot to advance toward the ball over uneven terrain while keeping the ball within its controllable range as much as possible.

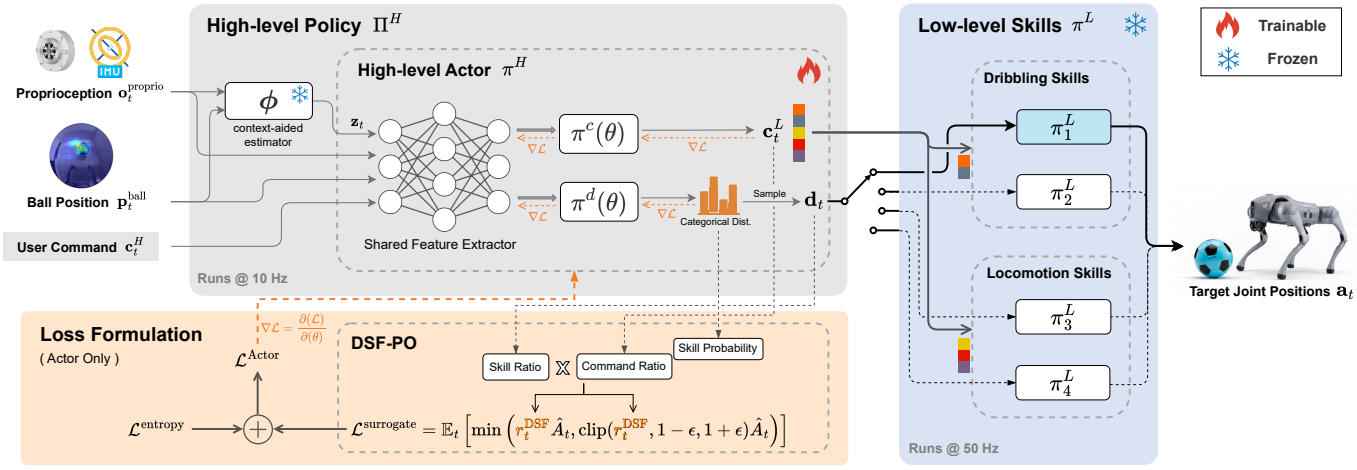

Fig. 2. **Hierarchical policy architecture and DSF-PO training paradigm.** A high-level policy running at 10 Hz consumes three types of observations to i) produce a categorical distribution over dribbling vs. locomotion skills and sample a skill index, and ii) output continuous command signals comprising both dribbling and locomotion commands. The actor's two heads share a feature extractor augmented by a frozen context-aided estimator. Pre-trained low-level skills execute at 50 Hz to track their respective subsets of high-level commands and generate the quadruped's target joint positions. Training optimizes the actor primarily with the DSF-PO loss, whose importance ratio is jointly modulated by the skill ratio and the skill probability. Value network is omitted for clarity.

We train these skills using PPO on both flat terrain (for π_3^L) and rugged terrain (for π_4^L). The terrain design for the latter follows the description in the *Environment Design* section of III-B2. Specifically, π_3^L is capable of moving at relatively high speeds on flat terrain, whereas π_4^L enables robust traversal over rough and sloped surfaces.

For each skill, the observation vector is

$$\left[\mathbf{c}_t^L,\ \mathbf{o}_t^{\text{proprio}},\ \boldsymbol{\theta}_t,\ (\mathbf{p}_t^{\text{ball}} \text{ if dribbling})\right],$$

where $\mathbf{c}_t^L$ denotes the low-level command, $\mathbf{p}^{\text{proprio}}$ is a subset of proprioceptive signals, and $\boldsymbol{\theta}_t$ is a timing reference variable following [5]. The proprioceptive subset includes joint positions and velocities $\mathbf{q}_t, \dot{\mathbf{q}}_t$, the gravity unit vector $\mathbf{g}_t$ in the body frame, and the global body yaw ψ_t. The command $\mathbf{c}_t^L$ encodes a target ball-velocity command $(v_x^{\text{cmd}}, v_y^{\text{cmd}})$ or a locomotion command $(v_x^{\text{cmd}}, v_y^{\text{cmd}}, \omega^{\text{cmd}})$. For dribbling skills, the ball position $\mathbf{p}^{\text{ball}}$ is additionally provided. Each policy outputs an action $\mathbf{a}_t \in \mathbb{R}^{12}$, interpreted as joint-position targets for the quadruped's twelve actuators, applied at 50 Hz.

2) High-level Policy: The high-level policy coordinates pre-trained low-level skills and orchestrates seamless transitions between dribbling and locomotion. Unlike [22], we adopt RL to train the high-level policy for robust ball-dribbling on rugged terrains. The high-level policy Π^H consists of a context-aided estimator ϕ and a high-level actor π^H (Fig. 2). The estimator ϕ provides structured, environment- and motion-related information to the actor. Specifically, it takes proprioception and ball position as input and predicts terrain parameters, the robot's posture, and the ball's motion states, yielding a compact context vector $\mathbf{z}_t$. Following [6], ϕ is trained with supervised learning using simulator ground truth and kept frozen during high-level policy training.

Observation Space: The high-level observation space $\mathbf{O}^H$ contains three components: proprioceptive signals, ball position, and user commands. The estimator ϕ processes the first two to produce $\mathbf{z}_t$, while the actor π^H consumes the full observation, i.e.,

$$\mathbf{o}_t = \left[\mathbf{z}_t,\ \mathbf{q}_t,\ \dot{\mathbf{q}}_t,\ \mathbf{g}_t,\ \psi_t,\ \ \mathbf{p}_t^{\text{ball}},\ \mathbf{c}_t^H,\ \ \mathbf{a}_{t-1}\right],$$

where $\mathbf{c}_t^H$ are user commands specifying the target ball velocity $\mathbf{v}_t^{\text{cmd}}$ in the global frame.

Action Space: The high-level actor π^H outputs a hybrid action $(d_t, \mathbf{c}_t^L)$, where $d_t \in \{1, \ldots, 4\}$ is a skill index and $\mathbf{c}_t^L \in \mathbb{R}^5$ is a partitioned command vector serving both 2D dribbling and 3D locomotion skills:

$$\mathbf{c}_t^L = \left[v_x^{\text{cmd}}, v_y^{\text{cmd}} \;\middle|\; v_x^{\text{cmd}}, v_y^{\text{cmd}}, \omega^{\text{cmd}}\right].$$

The appropriate sub-vector $\mathbf{c}_t^{d_t}$ is extracted via a skill-indexed selection matrix $\mathbf{S}_{d_t} \in \{\mathbf{S}_{\text{drib}}, \mathbf{S}_{\text{loc}}\}$, where the selection matrices are defined in block form as $\mathbf{S}_{\text{drib}} = [\ \mathbf{I}_2 \mid \mathbf{0}_{2\times 3}\ ]$ and $\mathbf{S}_{\text{loc}} = [\ \mathbf{0}_{3\times 2} \mid \mathbf{I}_3\ ]$. The selection is performed as:

$$\mathbf{c}_t^{d_t} = \mathbf{S}_{d_t}\mathbf{c}_t^L. \tag{6}$$

For locomotion skills $(d_t \in \{3, 4\})$, this command is then applied as a residual to the user command $\mathbf{c}_t^H$ with a scaling factor $\alpha \in (0, 1]$:

$$\tilde{\mathbf{c}}_t^{\text{loc}} = \mathbf{c}_t^H + \alpha\,\mathbf{c}_t^{d_t}. \tag{7}$$

Network Architecture: The actor network is specifically designed to handle a hybrid action space composed of a discrete skill index and a continuous command vector. As shown in Fig. 2, the architecture begins with a shared feature extractor, which is a three-layer MLP with [512,256,128] units and ELU activation functions. The output of the shared feature extractor is then fed into two distinct heads:

- The Skill Head π^d consists of a linear layer and softmax to produce a normalized four-dimensional categorical distribution, from which the skill index d_t is sampled.
- The Command Head π^c consists of a linear layer and *tanh* activation, generating a five-dimensional continuous

output within $(-1, 1)$. This output serves as the mean of a normal distribution $\mathcal{N}(\mu_t, \Sigma)$, from which the low-level commands $\mathbf{c}_t^L$ are sampled. The first two dimensions correspond to dribbling commands, and the remaining three correspond to locomotion commands.

Environment Design: We design five types of terrain — flat ground, ramp-up, ramp-down, rough terrain, and stair descent — to train the robot's ball dribbling ability in complex environments. At the start of every episode, the robot is randomly placed on one of these terrains with a random yaw orientation, and its joint angles are initialized around a nominal pose. The soccer ball is sampled within a $2\,\mathrm{m}$ radius of the robot. We adopt the domain randomization settings in [5]. User commands $\mathbf{c}_t^H$ are sampled via a curriculum, as detailed in Sec. III-C2.

C. Policy Training

In this section, we detail the training strategy for the high-level policy. To ensure efficient and stable learning, we introduce two key components: a novel loss formulation, Dynamic Skill-Focused Policy Optimization (DSF-PO), and a comprehensive training scheme involving reward shaping and curriculum learning.

1) Dynamic Skill-Focused Policy Optimization: As described in Sec. III-B2, the high-level policy, which selects low-level skills, mirrors Mixture-of-Experts (MoE) models like Switch Transformer [38] and introduces similar optimization challenges. Specifically, the high-level actor emits a hybrid action $(d_t, \mathbf{c}_t^L)$, where only the selected sub-vector $\mathbf{c}_t^{d_t}$ is actually executed by the environment. If one applies the vanilla PPO likelihood to the entire command vector, the log-probability decomposes across all skill-specific subspaces,

$$\log \pi_\theta \left(\mathbf{a}_t \mid \mathbf{s}_t\right) = \log \pi_\theta^d \left(d_t \mid \mathbf{s}_t\right) + \sum_{k=1}^{K} \log \pi_\theta^c \left(\mathbf{c}_t^k \mid \mathbf{s}_t, k\right), \tag{8}$$

so gradients can flow into $\pi^c(\cdot \mid \cdot, k)$ for $k \neq d_t$ — even though those commands were not executed. This creates an optimization-execution mismatch. To address this, we propose dynamic skill-focused policy optimization, a novel surrogate loss that focuses updates only on the parameters of the active skill.

Consider a high-level policy $\pi_\theta(\mathbf{a}|\mathbf{s})$ with two output heads: a discrete skill selector $\pi_\theta^d(d|\mathbf{s})$ and a continuous command generator $\pi_\theta^c(\mathbf{c}|\mathbf{s}, d)$. The skill selector samples $d \in \{1, \ldots, K\}$, while the command generator outputs $\mathbf{c}$, which is a union of different commands corresponding to each skill, $\mathbf{c} = \left(\mathbf{c}^1, \mathbf{c}^2, \ldots, \mathbf{c}^K\right)$, where $\mathbf{c}^k \in \mathbb{R}^{n_k}$ is the command for skill k. Once a skill d is selected, the low-level network processes only the corresponding command $\mathbf{c}^d$.

The action generation process begins with the skill selector which defines a categorical distribution over the K skills using softmax probabilities:

$$d \sim \text{Categorical}(p_1, \ldots, p_K),\ p_d = \pi_\theta^d(d|\mathbf{s}) = \frac{e^{z_d}}{\sum_{k=1}^{K} e^{z_k}}, \tag{9}$$

where z_d are the unnormalized logits. The command generator then provides the parameters for a multivariate normal distribution:

$$c^d \sim \mathcal{N}(\mu^d, \Sigma^d), \quad \mu^d = \pi_\theta^c(\mathbf{s}, d). \tag{10}$$

Thus, the overall policy $\pi_\theta(a|s)$ can be decomposed as:

$$\pi_\theta(\mathbf{a}|\mathbf{s}) = \pi_\theta^d(d|\mathbf{s}) \cdot \prod_{k=1}^{K} \mathcal{N}(\mathbf{c}^k; \mu_\theta^k, \Sigma^k)^{\mathbb{I}(k=d)}, \tag{11}$$

where $\mathbb{I}(k = d)$ is an indicator function that selects the appropriate command $\mathbf{c}^k$ based on the selected skill index d.

Let the skill focus weight be $w_k(\mathbf{s}) = \pi_\theta^d(k|\mathbf{s})$, representing the probability of selecting skill k given the state $\mathbf{s}$. The original importance ratio for policy optimization in PPO $r_t(\theta) = \frac{\pi_\theta(\mathbf{a}_t|\mathbf{s}_t)}{\pi_{\theta_{\text{old}}}(\mathbf{a}_t|\mathbf{s}_t)}$ can be written as:

$$r_t^{\text{DSF}}(\theta) = \underbrace{\frac{\pi_\theta^d(d_t|\mathbf{s}_t)}{\pi_{\theta_{\text{old}}}^d(d_t|\mathbf{s}_t)}}_{\text{Skill ratio}} \cdot \prod_{k=1}^{K} \left(\underbrace{\frac{\mathcal{N}(\mathbf{c}_t^k; \mu_\theta^k, \Sigma^k)}{\mathcal{N}(\mathbf{c}_t^k; \mu_{\theta_{\text{old}}}^k, \Sigma^k)}}_{\text{Command ratio}} \right)^{w_k(\mathbf{s}_t) \cdot \mathbb{I}(k=d_t)}. \tag{12}$$

The DSF-PO surrogate loss function can then be formulated as:

$$\mathcal{L}^{\text{surrogate}} = \mathbb{E}_t \left[\min \left(r_t^{\text{DSF}} \hat{A}_t, \text{clip}(r_t^{\text{DSF}}, 1-\epsilon, 1+\epsilon) \hat{A}_t \right) \right], \tag{13}$$

where $\hat{A}_t$ is the estimated advantage at time t and ϵ is the clipping parameter in PPO.

We employ PPO with Asymmetric Actor-Critic [39] to train the actor π^H of the high-level policy. The actor receives observations $\mathbf{o}_t$, while the value network (critic) gets the full state $\mathbf{s}_t$, which also includes the real velocities of the robot's base and the ball.

2) Reward Shaping and Curriculum Learning: We present a comprehensive training strategy inspired by [5] to deal with the challenges of skill switching and training stability in high-level ball dribbling control. To strike a balance in skill transitions, the high-level policy operates at a lower inference frequency (e.g., 10 Hz) than low-level skills. Additionally, we incorporate carefully designed reward terms and curriculum learning tailored to terrains and commands, as detailed in the following.

Reward Design: As the high-level policy should minimize its focus on the robot's low-level actions, the reward function is restricted to terms that are indispensable for stable learning, which consist of *five* components shown in Table I: 1) encouraging the robot to maintain its balance; 2) encouraging the robot to approach and orient toward the ball; 3) rewarding the consistent output of the same skill index $\mathbf{d_t}$ over time; 4) rewarding the proximity between the ball's actual and expected velocity; 5) encouraging the robot to use dribbling skills when approaching the ball. To ensure stable training, a bounded summation function is employed to aggregate all reward terms, with exponential kernels for weighted integration.

Curriculum Learning: To ensure stable from-scratch training of the high-level policy, we employ two curricula. The terrain curriculum progressively increases the steepness and

TABLE I
REWARD TERMS FOR HIGH-LEVEL POLICY TRAINING

Reinforcement Learning		
Term	Expression	Weight
Projected Gravity	$\lvert\mathbf{g}_{\text{xy}}\rvert^2$	-5.0
Robot Ball Distance	$\exp\{-\delta_p\lvert\mathbf{b}-\mathbf{p}_{\text{FRHip}}\rvert^2\}$	4.0
Yaw Alignment	$\exp\{-\delta_\psi(e^2_{\text{rbcmd}}+e^2_{\text{rbbase}})\}$	4.0
Temporal Coherence Bonus	$\sum_{i=t-T}^{t}\mathbb{I}(d_i=d_{i-1})$	0.1
Transition Cost	$\mathbb{I}(d_t\neq d_{t-1})$	-0.005
Ball Velocity Norm	$\exp\{-\delta_n(\lvert\mathbf{v}^{\text{cmd}}\rvert-\lvert\mathbf{v}^b\rvert)^2\}$	8.0
Ball Velocity Angle	$1-(\psi_b-\psi_{\text{cmd}})^2/\pi^2$	8.0
Ball Velocity Error	$\exp\{-\delta_v\lvert\mathbf{v}^b-\mathbf{v}^{\text{cmd}}\rvert^2\}$	8.0
Dribbling Near Ball	$\mathbb{I}(\lvert\mathbf{b}-\mathbf{p}\rvert<d_{\max})\cdot\mathbb{I}(\mathbf{d_t}\in\{1,2\})$	1.0
Curriculum Learning		
Term	Expression	
$r_{\mathbf{c}^H}$	$\mathbb{I}(r_{\text{BallVelocityError}}>0.5)$	
$r_{\mathbf{t}}$	$\mathbb{I}(\mathbf{b}>d_{\text{th1}})\cdot\mathbb{I}(\lvert\mathbf{b}-\mathbf{p}\rvert<d_{\text{th2}})$	

ruggedness of challenging environments (e.g., stairs, ramps, and rough terrains). Simultaneously, the command curriculum expands the range of user commands the robot must follow.

We define $p^k_{\mathbf{c}^H,\mathbf{t}}$ as the joint distribution of the user commands $\mathbf{c}^H$ and terrain difficulty $\mathbf{t}$ used in the sampling process during the k-th episode. An efficient approach is to maintain independent distributions over $p_{\mathbf{c}^H}, p_{\mathbf{t}}$ such that $p_{\mathbf{c}^H,\mathbf{t}} = p_{\mathbf{c}^H}\cdot p_{\mathbf{t}}$. Referring to [1], we employ the *box adaptive curriculum update rule* with a reward-based approach. Specifically, we initialize $p^0_{\mathbf{c}^H,\mathbf{t}}$ as a uniform probability distribution over $(\mathbf{c}^H\in[-0.5,0.5],\mathbf{t}\in\{0,1\})$. The user commands and terrain difficulty for the robot are sampled independently at episode k: $\mathbf{c}^H\sim p^k_{\mathbf{c}^H},\mathbf{t}\sim p^k_{\mathbf{t}}$. If the robot succeeds in this region, we will expand the sampling distribution to include neighboring regions, thereby increasing the task's difficulty. Suppose the robot receives rewards $r_{\mathbf{c}^H}$ and $r_{\mathbf{t}}$ for attempting to follow $\mathbf{c}^H$ and traverse the terrain with difficulty $\mathbf{t}$, respectively. We then apply the update rule:

$$p^{k+1}_{\mathbf{c}^H}\left(\mathbf{c}^H_{\text{n}}\right)\leftarrow\begin{cases}p^k_{\mathbf{c}^H}\left(\mathbf{c}^H_{\text{n}}\right) & \text{if } r_{\mathbf{c}^H}=1,\\ 1 & \text{otherwise.}\end{cases}\tag{14a}$$

$$p^{k+1}_{\mathbf{t}}\left(\mathbf{t}_{\text{n}}\right)\leftarrow\begin{cases}p^k_{\mathbf{t}}\left(\mathbf{t}_{\text{n}}\right) & \text{if } r_{\mathbf{t}}=1,\\ 1 & \text{otherwise.}\end{cases}\tag{14b}$$

Eq. (14) indicates the probability density on neighbors $\mathbf{c}^H_{\text{n}}$ of $\mathbf{c}^H$ and $\mathbf{t}_{\text{n}}$ of $\mathbf{t}$ are increased. For us, $\mathbf{c}^H_{\text{n}}\in\{\mathbf{c}^H-0.1,\mathbf{c}^H+0.1\},\mathbf{t}_{\text{n}}\in\{\mathbf{t}+1\}$. The reward terms are listed in Table I.

IV. RESULTS

In this section, we design both simulation studies and real-world experiments to evaluate the effectiveness of the proposed method and compare its ball dribbling performance on rugged terrains with previous approaches.

A. Experiment Results

1) Learning Performance: To validate the effectiveness of DSF-PO, we perform a detailed ablation study. Training is conducted in Isaac Gym, leveraging 4096 parallel environments on an NVIDIA RTX 4090. We compare our full DSF-PO formulation against two baselines by selectively ablating its key mechanisms:

- Vanilla PPO: This baseline removes both the skill focus weight and the indicator function:

$$r_t^{\text{vanilla}}(\theta)=\frac{\pi^d_\theta(d_t\mid\mathbf{s}_t)}{\pi^d_{\theta_{\text{old}}}(d_t\mid\mathbf{s}_t)}\cdot\prod_{k=1}^{K}\frac{\mathcal{N}\left(\mathbf{c}^k_t;\mu^k_\theta,\Sigma^k\right)}{\mathcal{N}\left(\mathbf{c}^k_t;\mu^k_{\theta_{\text{old}}},\Sigma^k\right)}\tag{15}$$

- DSF-PO (Focus-Only): This variant ablates the skill focus weight but retains the indicator function:

$$r_t^{\text{Focus-Only}}(\theta)=\frac{\pi^d_\theta(d_t\mid\mathbf{s}_t)}{\pi^d_{\theta_{\text{old}}}(d_t\mid\mathbf{s}_t)}\cdot\frac{\mathcal{N}(\mathbf{c}^{d_t}_t;\mu^{d_t}_\theta,\Sigma^{d_t})}{\mathcal{N}(\mathbf{c}^{d_t}_t;\mu^{d_t}_{\theta_{\text{old}}},\Sigma^{d_t})}\tag{16}$$

All runs use PPO with standard legged-robot hyperparameters (Table II), identical across DSF-PO and other ablations. Fig. 3 shows the learning curves: the full DSF-PO consistently surpasses vanilla PPO, achieving higher return and longer episodes with faster early improvement. The *Focus-Only* ablation briefly outperforms vanilla PPO but saturates below DSF-PO, indicating that adaptive, skill-aware optimization improves both sample efficiency and final performance.

2) Terrain Traversability: To evaluate the terrain traversability, we conduct two comparative studies. First, we compare the learned policy with DribbleBot [5] and DexDribbler [6]. Two baseline-oriented tasks are also included: i) fine-tuning the baselines on the environment introduced in Sec. III-B2, and ii) training the baselines from scratch under the same environment. Because the publicly released checkpoints of baselines were trained with the Unitree Go1, all evaluations are conducted using the Go1 model to ensure a fair comparison. All policies

TABLE II
HYPER-PARAMETERS FOR HIGH-LEVEL POLICY TRAINING

Hyperparameter	Value
Rollout buffer size	24 steps
Discount factor (γ)	0.99
GAE parameter (λ)	0.95
PPO clipping ratio (ϵ)	0.2
Number of epochs per update	5
Minibatch size	4
Optimizer	Adam
Learning rate	1×10^{-3}
Entropy coefficient	0.01
Value function coefficient	1.0

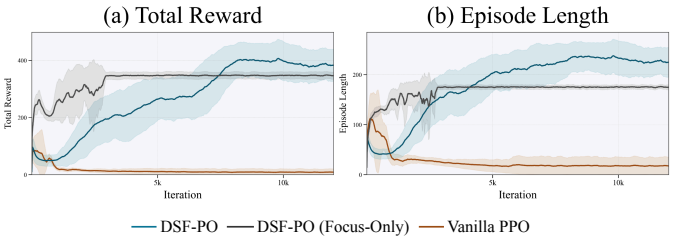

Fig. 3. Training curves of PPO with DSF-PO compared to vanilla PPO and DSF-PO with focus only. The shaded regions indicate the standard deviation over multiple runs.

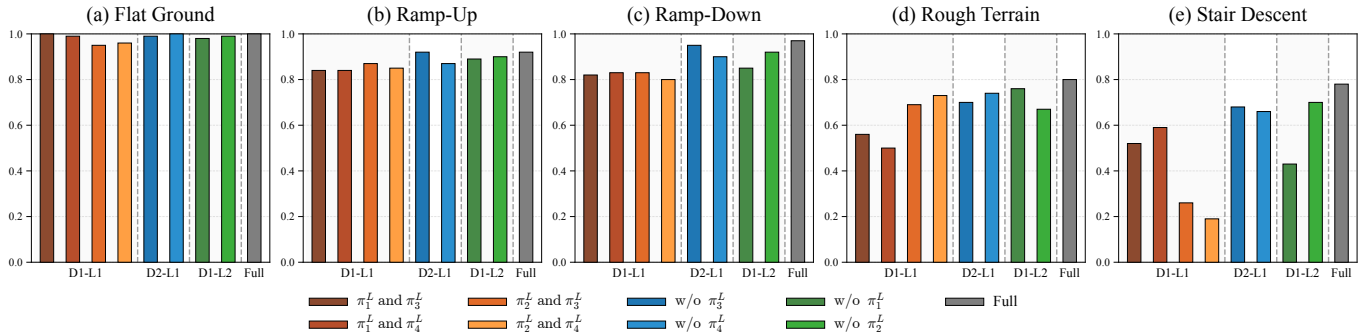

Fig. 4. **Low-level skill ablation across terrains.** Each panel shows per-terrain success rates based on 100 trials. Groups D1–L1, D2–L1, D1–L2, and Full denote the numbers of dribbling (D) and locomotion (L) skills: $(D, L) = (1, 1)$, $(2, 1)$, $(1, 2)$, $(2, 2)$.

TABLE III
BALL DRIBBLING SUCCESS RATES ACROSS DIFFERENT TERRAINS

Method	Flat Ground	Ramp-Up	Ramp-Down	Rough Terrain	Stair Descent
DribbleBot	**1.00**	0.89	0.90	0.53	0.61
DribbleBot-FT[1]	**1.00**	0.65	0.76	0.62	0.36
DribbleBot-S[2]	0.10	0.03	0.01	0.00	0.00
DexDribbler	**1.00**	0.91	0.92	0.22	0.13
DexDribbler-FT	**1.00**	0.90	0.93	0.30	0.08
DexDribbler-S	0.15	0.07	0.10	0.01	0.00
Ours	**1.00**	**0.92**	**0.97**	**0.80**	**0.78**

* Terrain settings: ramp-up ($m = 0.10$); ramp-down ($m = -0.10$); rough terrain ($\Delta h = 0.10\,\mathrm{m}$); stair descent ($h = 0.05\,\mathrm{m}, d = 0.50\,\mathrm{m}$).
[1] The suffix *FT* indicates the algorithm was fine-tuned on above terrains.
[2] The suffix *S* indicates the algorithm was trained from scratch on above terrains.

are tested under the same command: $\mathbf{c}_t = (1.0, 0.0)$. We conduct 100 tests per method on each terrain, where success is defined as the robot reaching the terrain boundary. As shown in Table III, most methods achieve 100% on flat ground, whereas performance diverges on harder terrains; our approach attains the best success rates on all non-flat settings. For the baselines, fine-tuning on the complex terrain yields at most marginal gains and sometimes substantial declines, and training from scratch on these terrains performs even worse than their flat-trained counterparts. These results indicate that a single monolithic RL policy is insufficient for robust operation on complex terrains.

Second, we perform an ablation study fon low-level skill combinations. Combinations are grouped into four categories: i) D1–L1, one dribbling and one locomotion skill; ii) D2–L1, two dribbling and one locomotion skill; iii) D1–L2, one dribbling and two locomotion skills; and iv) Full, the proposed 2D–2L composition. Success rates for all nine combinations are evaluated across five terrains under the same protocol as above. As shown in Fig. 4, performance increases with low-level capacity: D1–L1 degrades on rough terrain and stairs; adding a second dribbling or locomotion skill (D2–L1/D1–L2) yields consistent gains, and the Full 2D–2L setting is most reliable across all terrains, indicating that capacity and complementary skills drive traversability.

3) Cross-Terrain Dribbling: As shown in Fig. 5, we evaluate the robot's dribbling ability across five terrains: stair descent, ramp-down, rough terrain, ramp-up, and flat ground. With a fixed command $\mathbf{c}_t^H = (1.0, 0.0)$, the robot successfully completes the task in 121 seconds. It maintains a stable direction except on rough terrain, where external disturbances cause deviations. Fig. 5(b) shows the invocation of low-level skills by the high-level policy across different terrains. The results indicate that dribbling skills are used most frequently, allowing the policy to adaptively switch between them based on terrain variations. Locomotion skills are invoked less frequently, mainly when the robot needs to reposition itself after drifting away from the ball. Fig. 5(c) and 5(d) illustrate the ball's velocity magnitude and direction, respectively. On downhill terrains (stair descent, ramp-down), the robot struggles to precisely control the ball's velocity due to gravitational acceleration. Velocity fluctuations are pronounced on rough terrain, mainly due to uneven surfaces. In contrast, on ramp-up and flat ground, the robot effectively regulates the ball's velocity, demonstrating greater stability and control.

Notably, the high-level policy selects π_2^L with high frequency, although the method from which π_2^L originates (DexDribbler) underperforms on rough terrain and stair descent (shown in Table III). This apparent discrepancy is attributable to the integration of π_2^L within our hierarchical controller and the presence of complementary skills, which together enhance contact negotiation, thereby enabling robust traversability on challenging terrains.

4) Modality-Skill Consistency: We assess whether the high-level skill selection aligns with the contact modality indicated by the impulse-based contact flag $i_t \in \{0, 1\}$: dribbling skills $\mathcal{D} = \{1, 2\}$ are expected under contact (i_t=1) and locomotion skills $\mathcal{L} = \{3, 4\}$ are expected under non-contact (i_t=0). From the trajectory in Fig. 5, we construct a confusion matrix between the contact label i_t and the predicted skill category $d_t \in \{\mathcal{D}, \mathcal{L}\}$. The matrix is row-normalized and summarized by two scalar metrics reported in Table IV: balanced accuracy (BAcc) and Matthews correlation (MCC). BAcc captures average correctness under class imbalance (good if ≥ 0.80, very strong if ≥ 0.90), while MCC (-1 to 1) reflects overall agreement (strong if ≥ 0.70). In our data, $\mathrm{BAcc} = 0.866$ and $\mathrm{MCC} = 0.727$, indicating strong, well-balanced alignment: the selector reliably switches to $\mathcal{D}$ upon contact and maintains $\mathcal{L}$ otherwise.

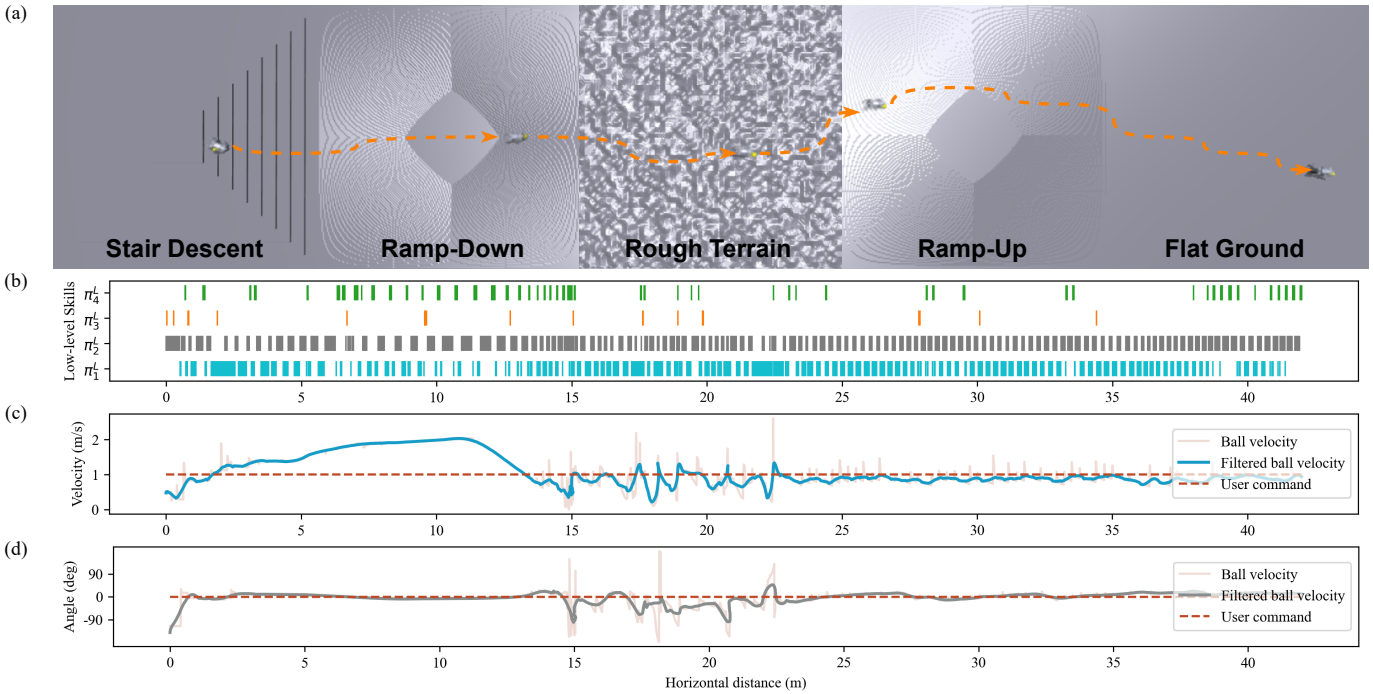

Fig. 5. **Cross-terrain dribbling performance evaluation.** (a) A trajectory schematic of the ball dribbling across five terrains in sequence. Each terrain measures 10 m per side. (b) Visualization of the invocation of different low-level skills, where each thin vertical line represents a single invocation. (c-d) Visualization of the ball's velocity magnitude and direction. The horizontal axis represents the robot's traveled horizontal distance.

TABLE IV
ROW-NORMALIZED CONFUSION MATRIX AND METRICS OF MODALITY–SKILL CONSISTENCY

Actual i_t	**Predicted** d_t		BAcc	MCC
	$\mathcal{D}$ (dribbling)	$\mathcal{L}$ (locomotion)		
1 (contact)	0.897	0.103	0.866	0.727
0 (no contact)	0.166	0.834		

TABLE V
REAL WORLD BALL DRIBBLING PERFORMANCE EVALUATION

Method	Ramp-Up	Ramp-Down	Gravel	Stair Descent
DribbleBot	0/4	0/4	**4/4**	–
DexDribbler	**4/5**	1/5	**5/5**	–
Ours	**4/5**	**3/5**	**5/5**	**3/5**

B. Physical Deployment

We deploy on a Unitree Go2 quadruped equipped with a downward-facing fisheye camera (240° field of view) mounted on the head; all inference runs onboard on an NVIDIA Jetson Orin NX. A YOLOv11 detector provides ball observations, which are converted to metric distances using the equidistant fisheye model $r = f\theta$. We compute 2D ball coordinates via two geometric solvers (one from apparent diameter, one from angle–range) and fuse them with a Kalman filter. For control, we use a PD controller with k_p=20, k_d=0.5 during training and evaluation; the rough-terrain locomotion skill π_4^L uses k_p=40, k_d=1.0 to improve passability. All policies are transferred to the physical robot in a zero-shot manner, which proved effective in our setup.


(a) Ramp-Up


(b) Ramp-Down

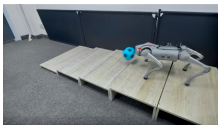
(c) Stair Descent


(d) Cross-Terrain

Fig. 6. **Real-world deployment experiments on different terrains.** The indoor environment includes ramp-up, ramp-down, and stair descent, while the outdoor environment consists of a complex multi-terrain field.

We evaluate on four terrains (Fig. 6): ramp-up, ramp-down, stair descent (each step 50 cm wide, 5 cm high), and cross-terrain (mixed irregular ground, raised curbs, smooth stone pavement, soft gravel). The robot and ball start on flat ground and the objective is to drive the ball to the far end while maintaining balance. High-level commands are published via a remote controller. We conduct five trials per terrain; statistics are reported in Table V. The baseline results are directly extracted from the corresponding original papers to ensure a fair and consistent comparison.

Across all four terrains, our method attains the highest

success rate, indicating stronger generalization. Qualitatively, the high-level policy adapts skill usage to terrain: on flat ground it maintains steady dribbling; on ramps it adjusts posture and limb coordination to counter slope while stabilizing ball control; on stairs it first kicks the ball down steps and then follows under stabilized gait; on rough outdoor ground it modulates stride length and stance width while switching skills to sustain stable dribbling.

V. Conclusion

In this paper, we propose a hierarchical RL framework that trains a high-level policy to coordinate dribbling and locomotion skills for dynamic ball manipulation on rugged terrains. We also introduce a dynamic skill-focused loss formulation to improve learning efficiency and convergence in mixed discrete-continuous action spaces. Simulation and real-world experiments show that our methods outperform previous works in generalizing across diverse terrains, achieving stable ball dribbling performance on rugged surfaces. Moreover, the framework is highly scalable, allowing the integration of more low-level skills to tackle complex tasks and diverse motion modalities. Future work will be devoted to extending low-level inputs to 3D to reduce positional ambiguity on uneven terrain, and to integrating additional multimodal skills within our hierarchical RL framework to enhance autonomy.

References

[1] G. B. Margolis, G. Yang, K. Paigwar, T. Chen, and P. Agrawal, "Rapid locomotion via reinforcement learning," *The International Journal of Robotics Research*, 2024.

[2] Z. Zhuang, Z. Fu, J. Wang, C. Atkeson, S. Schwertfeger, C. Finn, and H. Zhao, "Robot parkour learning," in *CoRL*, 2023.

[3] Y. Ji, Z. Li, Y. Sun, X. B. Peng, S. Levine, G. Berseth, and K. Sreenath, "Hierarchical reinforcement learning for precise soccer shooting skills using a quadrupedal robot," in *IROS*, 2022.

[4] S. Ha, J. Lee, M. van de Panne, Z. Xie, W. Yu, and M. Khadiv, "Learning-based legged locomotion: State of the art and future perspectives," *The International Journal of Robotics Research*, 2024.

[5] Y. Ji, G. B. Margolis, and P. Agrawal, "Dribblebot: Dynamic legged manipulation in the wild," in *ICRA*, 2023.

[6] Y. Hu, K. Wen, and F. Yu, "Dexdribbler: Learning dexterous soccer manipulation via dynamic supervision," in *IROS*, 2024.

[7] R. Huang, S. Zhu, Y. Du, and H. Zhao, "Moe-loco: Mixture of experts for multitask locomotion," in *IROS*, 2025.

[8] K. Jiang, Z. Fu, J. Guo, W. Zhang, and H. Chen, "Learning whole-body loco-manipulation for omni-directional task space pose tracking with a wheeled-quadrupedal-manipulator," *IEEE Robotics and Automation Letters*, 2025.

[9] S. Jeon, M. Jung, S. Choi, B. Kim, and J. Hwangbo, "Learning whole-body manipulation for quadrupedal robot," *IEEE Robotics and Automation Letters*, 2024.

[10] Y. Kim, H. Oh, J. Lee, J. Choi, G. Ji, M. Jung, D. Youm, and J. Hwangbo, "Not only rewards but also constraints: Applications on legged robot locomotion," *IEEE Transactions on Robotics*, 2024.

[11] G. Pan *et al.*, "Roboduet: Learning a cooperative policy for whole-body legged loco-manipulation," *IEEE Robotics and Automation Letters*, 2025.

[12] G. Ji, J. Mun, H. Kim, and J. Hwangbo, "Concurrent training of a control policy and a state estimator for dynamic and robust legged locomotion," *IEEE Robotics and Automation Letters*, 2022.

[13] J. Cheng, D. Kang, G. Fadini, G. Shi, and S. Coros, "Rambo: Rl-augmented model-based whole-body control for loco-manipulation," *IEEE Robotics and Automation Letters*, 2025.

[14] I. M. A. Nahrendra, B. Yu, and H. Myung, "Dreamwaq: Learning robust quadrupedal locomotion with implicit terrain imagination via deep reinforcement learning," in *ICRA*, 2023.

[15] H. Zhang, H. Yu, L. Zhao, A. Choi, Q. Bai, Y. Yang, and W. Xu, "Learning multi-stage pick-and-place with a legged mobile manipulator," *IEEE Robotics and Automation Letters*, 2025.

[16] J. Hwangbo, J. Lee, A. Dosovitskiy, D. Bellicoso, V. Tsounis, V. Koltun, and M. Hutter, "Learning agile and dynamic motor skills for legged robots," *Science Robotics*, 2019.

[17] J. Lee, J. Hwangbo, L. Wellhausen, V. Koltun, and M. Hutter, "Learning quadrupedal locomotion over challenging terrain," *Science Robotics*, 2020.

[18] N. Rudin, D. Hoeller, P. Reist, and M. Hutter, "Learning to walk in minutes using massively parallel deep reinforcement learning," in *CoRL*, 2022.

[19] T. Miki, J. Lee, J. Hwangbo, L. Wellhausen, V. Koltun, and M. Hutter, "Learning robust perceptive locomotion for quadrupedal robots in the wild," *Science Robotics*, 2022.

[20] G. B. Margolis and P. Agrawal, "Walk these ways: Tuning robot control for generalization with multiplicity of behavior," in *CoRL*, 2023.

[21] P. Arm, M. Mittal, H. Kolvenbach, and M. Hutter, "Pedipulate: Enabling manipulation skills using a quadruped robot's leg," in *ICRA*, 2024.

[22] X. Cheng, A. Kumar, and D. Pathak, "Legs as manipulator: Pushing quadrupedal agility beyond locomotion," in *ICRA*, 2023.

[23] X. Huang, Z. Li, Y. Xiang, Y. Ni, Y. Chi, Y. Li, L. Yang, X. B. Peng, and K. Sreenath, "Creating a dynamic quadrupedal robotic goalkeeper with reinforcement learning," in *IROS*, 2023.

[24] Z. He, K. Lei, Y. Ze, K. Sreenath, Z. Li, and H. Xu, "Learning visual quadrupedal loco-manipulation from demonstrations," in *IROS*, 2024.

[25] X. Huang, Q. Liao, Y. Ni, Z. Li, L. Smith, S. Levine, X. B. Peng, and K. Sreenath, "Hilma-res: A general hierarchical framework via residual rl for combining quadrupedal locomotion and manipulation," in *IROS*, 2024.

[26] D. Precup, *Temporal abstraction in reinforcement learning*. University of Massachusetts Amherst, 2000.

[27] O. Nachum, S. Gu, H. Lee, and S. Levine, "Near-optimal representation learning for hierarchical reinforcement learning," in *ICLR*, 2019.

[28] M. Hutsebaut-Buysse, K. Mets, and S. Latré, "Hierarchical reinforcement learning: A survey and open research challenges," *Machine Learning and Knowledge Extraction*, 2022.

[29] X. B. Peng, G. Berseth, K. Yin, and M. Van De Panne, "Deeploco: Dynamic locomotion skills using hierarchical deep reinforcement learning," *ACM Trans. Graph.*, 2017.

[30] D. Jain, A. Iscen, and K. Caluwaerts, "Hierarchical reinforcement learning for quadruped locomotion," in *IROS*, 2019.

[31] W. Tan, X. Fang, W. Zhang, R. Song, T. Chen, Y. Zheng, and Y. Li, "A hierarchical framework for quadruped omnidirectional locomotion based on reinforcement learning," *IEEE Transactions on Automation Science and Engineering*, 2023.

[32] J. Gehring, G. Synnaeve, A. Krause, and N. Usunier, "Hierarchical skills for efficient exploration," in *NeurIPS*, 2021.

[33] X. Yang, Z. Ji, J. Wu, Y.-K. Lai, C. Wei, G. Liu, and R. Setchi, "Hierarchical reinforcement learning with universal policies for multi-step robotic manipulation," *IEEE Transactions on Neural Networks and Learning Systems*, 2021.

[34] K. N. Kumar, I. Essa, and S. Ha, "Cascaded compositional residual learning for complex interactive behaviors," *IEEE Robotics and Automation Letters*, 2023.

[35] N. Yokoyama, A. Clegg, J. Truong, E. Undersander, T.-Y. Yang, S. Arnaud, S. Ha, D. Batra, and A. Rai, "Asc: Adaptive skill coordination for robotic mobile manipulation," *IEEE Robotics and Automation Letters*, 2023.

[36] J. Schulman, F. Wolski, P. Dhariwal, A. Radford, and O. Klimov, "Proximal policy optimization algorithms," *arXiv preprint arXiv:1707.06347*, 2017.

[37] V. Makoviychuk *et al.*, "Isaac gym: High performance GPU based physics simulation for robot learning," in *Thirty-fifth Conference on Neural Information Processing Systems Datasets and Benchmarks Track (Round 2)*, 2021.

[38] W. Fedus, B. Zoph, and N. Shazeer, "Switch transformers: Scaling to trillion parameter models with simple and efficient sparsity," *Journal of Machine Learning Research*, 2022.

[39] L. Pinto, M. Andrychowicz, P. Welinder, W. Zaremba, and P. Abbeel, "Asymmetric actor critic for image-based robot learning," in *Robotics: Science and Systems*, 2018.